Computational and Structural Biotechnology Journal 23 (2024) 369–383

Contents lists available at ScienceDirect

Computational and Structural Biotechnology Journal

journal homepage: www.elsevier.com/locate/csbj

Research article

Inflammatory response signature score model for predicting immunotherapy response and pan-cancer prognosis

Shuzhao Chen [a,b,1], Mayan Huang [c,1], Limei Zhang [a,1], Qianqian Huang [a,1], Yun Wang [a,*], Yang Liang [a,*]

[a] Department of Hematologic Oncology, Sun Yat-sen University Cancer Center, State Key Laboratory of Oncology in South China, Collaborative Innovation Center for Cancer Medicine, Guangdong Provincial Clinical Research Center for Cancer, Guangzhou, Guangdong, China
[b] Department of Thyroid and Breast Surgery, Clinical Research Center, The First Affiliated Hospital of Shantou University Medical College (SUMC), Shantou, Guangdong, China
[c] Department of Pathology, Sun Yat-Sen University Cancer Center, Guangzhou, Guangdong, China

ARTICLE INFO

Keywords:
Cancer immunotherapy response
Inflammatory response
Tumor immunity
Biomarker

ABSTRACT

Background: Inflammatory responses influence the outcome of immunotherapy and tumorigenesis by modulating host immunity. However, systematic inflammatory response assessment models for predicting cancer immunotherapy (CIT) responses and survival across human cancers remain unexplored. Here, we investigated an inflammatory response score model to predict CIT responses and patient survival in a pan-cancer analysis.

Methods: We retrieved 12 CIT response gene expression datasets from the Gene Expression Omnibus database (GSE78220, GSE19423, GSE100797, GSE126044, GSE35640, GSE67501, GSE115821 and GSE168204), Tumor Immune Dysfunction and Exclusion database (PRJEB23709, PRJEB25780 and phs000452.v2.p1), European Genome-phenome Archive database (EGAD00001005738), and IMvigor210 cohort. The tumor samples from six cancers types: metastatic urothelial cancer, metastatic melanoma, gastric cancer, primary bladder cancer, renal cell carcinoma, and non-small cell lung cancer.

We further established a binary classification model to predict CIT responses using the least absolute shrinkage and selection operator (LASSO) computational algorithm.

Findings: The model had high predictive accuracy in both the training and validation cohorts. During sub-group analysis, area under the curve (AUC) values of 0.82, 0.80, 0.71, 0.7, 0.67, and 0.64 were obtained for the non-small cell lung cancer, gastric cancer, metastatic urothelial cancer, primary bladder cancer, metastatic melanoma, and renal cell carcinoma cohorts, respectively. CIT response rates were higher in the high-scoring training cohort subjects (51%) than the low-scoring subjects (27%). The five-year survival rates in the high- and low score groups of the training cohorts were 62% and 21%, respectively, while those of the validation cohorts were 54% and 22%, respectively ($P < 0{\cdot}001$ in all cases). Inflammatory response signature score derived from on-treatment tumor specimens are highly predictive of response to CIT in patients with metastatic melanoma. A significant correlation was observed between the inflammatory response scores and tumor purity. Regardless of the tumor purity, patients in the low score group had a significantly poorer prognosis than those in the high score group. Immune cell infiltration analysis indicated that in the high score cohort, tumor-infiltrating lymphocytes were significantly enriched, particularly effector and natural killer cells. Inflammatory response scores were positively correlated with immune checkpoint genes, suggesting that immune checkpoint inhibitors may have benefited patients with high scores. Analysis of signature scores across different cancer types from The Cancer Genome Atlas revealed that the prognostic performance of inflammatory response scores for survival in patients who have not undergone immunotherapy can be affected by tumor purity. Interleukin 21 (IL21) had the highest weight in the inflammatory response model, suggesting its vital role in the prediction mode. Since the number of metastatic melanoma patients (n = 429) was relatively large among CIT cohorts, we further performed a co-culture experiment using a melanoma cell line and CD8 + T cell populations generated from peripheral blood monocytes. The results showed that IL21 therapy combined with anti-PD1 (programmed cell death 1) antibodies

* Corresponding authors.
E-mail addresses: wangyun@sysucc.org.cn (Y. Wang), liangyang@sysucc.org.cn (Y. Liang).
[1] These authors contributed equally: Shuzhao Chen, Mayan Huang, Limei Zhang, Qianqian Huang

https://doi.org/10.1016/j.csbj.2023.12.001
Received 9 June 2023; Received in revised form 29 November 2023; Accepted 2 December 2023
Available online 6 December 2023

(trepril monoclonal antibodies) significantly enhanced the cytotoxic activity of CD8 + T cells against the melanoma cell line.

Conclusion: In this study, we developed an inflammatory response gene signature model that predicts patient survival and immunotherapy response in multiple malignancies. We further found that the predictive performance in the non-small cell lung cancer and gastric cancer group had the highest value among the six different malignancy subgroups. When compared with existing signatures, the inflammatory response gene signature scores for on-treatment samples were more robust predictors of the response to CIT in metastatic melanoma.

1. Introduction

Cancer immunotherapy (CIT; adoptive cell transfer (ACT) [1], melanoma antigen family A3 (MAGE A3) [2] therapy, *Bacillus* Calmette—Guérin (BCG) immunotherapy [3], and immune checkpoint inhibitor (ICI) therapy [4]), has improved outcomes for patients with various types of cancers. However, the majority of patients do not derive long-term benefits from or achieve a durable clinical response to these therapies. Moreover, strong and concise predictive biomarkers to guide CIT are lacking, which has hindered the classification of patients into responsive and non-responsive categories and caused the overuse of CIT, which introduces associated costs and unnecessary potential side effects. Therefore, there is an urgent need to develop a parsimonious prediction model that can assess patient response to CIT to identify those who may benefit.

Previous studies have identified gene signatures in CIT responses. For example, Xiong et al. identified and validated a signature (including 108 genes) called ImmuneCells.Sig, which is enriched in genes associated with the triggering receptor expressed on myeloid cells 2 (TREM2) receptor in macrophages, γδ T cells, and B cell subpopulations. [5] Loss of major histocompatibility complex class I (MHC-I) can predict primary resistance to anti-CTLA-4 therapy [6], and melanoma-specific MHC class II gene expression predicts response to anti-PD-1/PD-L1 therapy. [7] Ju et al. revealed the potential application of the NLRP3 inflammasome signature (including 30 genes) as a predictive biomarker of immunotherapy response. [8] Ayers et al. reported a T-cell-–inflamed gene expression signature (including 18 genes) that can be used to identify PD-1 checkpoint blockade-responsive biology and predict clinical response across a variety of tumor types, including bladder, gastric, head and neck squamous cell carcinoma, triple-negative breast cancer, anal canal, biliary, colorectal, esophageal, and ovarian cancers. [9] In our previous studies, we found that the glycoprotein VI-mediated platelet activation signaling pathway signature (including 35 genes) scores were robust predictors of the response to anti-PD-1 blockade in metastatic melanoma [10]. We also identified four functional gene signatures associated with the endothelium, effector cells, B cells, and tumor proliferation rate that accurately predict the response of metastatic melanoma patients to immune checkpoint blockade (ICB) therapy [11]. However, gene expression profiles are not widely used in clinical practice because of the lack of reproducibility associated with various array platforms and interpretative methods. Thus, accurate biomarkers for predicting patient survival and CIT responses have not been identified.

Inflammation can affect immune cell infiltration and response to therapy. Inflamed tumors are characterized by the enrichment of tumor-infiltrating T cells, such as CD4 + and CD8 + T-cells. [12] These immune cells are frequently found adjacent to the tumor cells. Furthermore, many effector cytokines can be detected at the transcriptome level in inflamed tumors. [13] Immunohistochemistry analyses have suggested that programmed cell death 1 ligand 1 (PDL1) is expressed on tumor-infiltrating immune cells or tumor cells, [14] which indicates that a pre-existing antitumor immune response occurs in the inflammatory environment within tumor tissue. Indeed, anti-PDL-1/PD-1 therapy has shown a more effective response in patients with an inflamed tumor microenvironment than in patients without such a microenvironment. [15,16] This indicates that inflammatory response-related genes can be involved in immunotherapy for various cancer types. However, whether inflammatory response genes can serve as predictive biomarkers of the CIT response requires further investigation.

In this study, we aimed to develop an inflammatory response score model to predict immunotherapy response. Data for the model were obtained from public datasets of inflammatory response-related genes across six cancer types, including non-small cell lung cancer, gastric cancer, metastatic urothelial cancer, primary bladder cancer, metastatic melanoma, and renal cell carcinoma.

2. Methods

2.1. Studies and patient selection

We systematically retrieved the publicly database to identify eligible gene expression datasets with information on immunotherapy response in subjects with solid malignancies. Criteria for inclusion were as follows: (a). All patients with a confirmed diagnosis of solid malignancies; (b). All patients were received immunotherapy; (c). All patients with treatment response information; (d). All data were publicly available and usable. Finally, the 12 published CIT response datasets was selected (Table S1). The Hugo et al. (GSE78220) [17], Kim et al. (GSE19423) [3], Lauss et al. (GSE100797) [1], Cho et al. (GSE126044) [18], Ulloa-Montoya et al. (GSE35640) [2], Ascierto et al. (GSE67501) [19], and MGH datasets (GSE115821 [20] and GSE168204 [21]) were downloaded from the Gene Expression Omnibus database (http://www.ncbi.nlm.nih.gov/geo/). The Gide et al. (PRJEB23709) [22], Kim et al. (PRJEB25780) [23], and Van Allen et al. datasets (phs000452.v2. p1) [24] were obtained from the Tumor Immune Dysfunction and Exclusion database (http://tide.dfci.harvard.edu/) [25]. The Lee et al. dataset (EGAD00001005738) [26] was downloaded from the European Genome-phenome Archive database (https://ega-archive.org/access/data-access/) [27]. The IMvigor210 cohort [28] data were obtained using the IMvigor210CoreBiologies package for R software. A robust multi-array quantile method was then employed to normalize the data from the different arrays [29]. Patient responses to CIT were assessed according to the Response Evaluation Criteria in Solid Tumors (https://recist.eortc.org/). Details on the immunotherapy response datasets are provided in Table S1, and a summary of the study is provided in Fig. S1.

RNA-Seq by Expectation Maximization data and clinical information for the 20 cohorts from The Cancer Genome Atlas (TCGA) were downloaded from TCGA PanCanAtlas [30], which is available at https://gdc.cancer.gov/about-data/publications/pancanatlas. More than 7000 tumor samples were selected after filtering out samples that lacked clinical survival information (n = 54). All TCGA abbreviations are shown in Table S2.

The inflammatory response Gene Ontology (GO) dataset (GO:0006954) for *Homo sapiens* containing 851 genes was chosen from Gene Ontology Browser (https://www.informatics.jax.org/vocab/gene_ontology) by searching the keyword "inflammatory response." A similar dataset containing 854 genes for Gene Set Enrichment Analysis (GSEA) [31] (GOBP_INFLAMMATORY_RESPONSE) was obtained from the MSigDB dataset (https://www.gsea-msigdb.org/gsea/msigdb). Finally, 808 genes common to both these datasets, which were annotated by the respective GO (GO:0006954) and GSEA (GOBP_INFLAMMATORY_RESPONSE) categories, were selected for further

downstream analysis.

2.2. Construction and validation of inflammatory response scores

Coefficient profiles of the 808 inflammatory response genes were selected based on Least Absolute Shrinkage and Selection Operator (LASSO) binomial logistic regression model analysis. [32] The inflammatory response score model used a 10-fold cross-validation estimator to penalize the maximum-likelihood estimation. Data from 784 patients who underwent CIT were randomly partitioned into training (70%) and validation (30%) sets. The predict.glm function was used to employ the logistic regression model for the training and validation cohort data. Inflammatory response signatures were generated according to the training cohort data, and the ability of these signatures to predict CIT response was evaluated based on the testing and overall cohort (including training and testing groups).

The inflammatory response score was calculated as follows:

$$Scores = \sum_{i=1}^{n} \exp_i * \beta_i$$

where n, $\exp_i$, and β represent the number of genes, mRNA expression value, and the LASSO coefficient of gene i, respectively. The expression values were normalized across the datasets using the robust multi-array quantile method.

Patients with metastatic melanoma undergoing CIT were singled out and further divided into on-treatment and pre-treatment cohorts to verify the predictive power of the inflammatory response signature. Data from the metastatic urothelial cancer cohort were sufficient for independent analyses of the inflammatory response based on the multivariable Cox regression method.

2.3. Gene set enrichment analysis

Using the clusterProfiler package, the potential biological functions associated with inflammatory response scores between the low-scoring and high-scoring groups of each cancer type were determined using the GSEA tool. [33] The curated gene sets (h.all.v7.2.symbols.gmt and c2.cp.reactome.v7.5.1.symbols.gmt) can be obtained from the GSEA website (http://www.gsea-msigdb.org/gsea/downloads.jsp). Statistical significance was defined at a p-value threshold of 0.05.

2.4. Immunity analysis and gene expression

The Estimation of Stromal and Immune cells in Malignant Tumor tissues using Expression data (ESTIMATE) [34], Estimating the Proportions of Immune and Cancer cells (EPIC) [35], Microenvironment Cell Populations-counter (MCPcounter) [36], Immune Cell Abundance Identifier (ImmuCellAI) [37], CIBERSORT [38], xCell [39], tumor immune estimation resource (TIMER) [40], and Single-sample Gene Set Enrichment Analysis (ssGSEA) [41] algorithms were used to assess the cellular component or cellular immune response profiles between the high- and low-score groups. ESTIMATE is an algorithm that uses gene expression signatures to infer the fraction of stromal and immune cells in tumor samples [34]. EPIC estimates the proportions of immune and cancer cells using RNA-seq-based gene expression reference profiles from immune cells and other nonmalignant cell types found in tumors. [35] MCPcounter estimates the immune and stromal composition of heterogeneous tissue based on transcriptomic data [36]. ImmuCellAI precisely estimates the abundance of 24 immune cell types, including 18 T-cell subsets, based on gene set characteristics. [37] CIBERSORT imputes gene expression profiles and provides estimates of the abundance of member cell types in a mixed cell population using gene expression data [38]. The novel xCell method was used to infer 64 immune and stromal cell types based on gene signatures [39]. TIMER is a comprehensive database for systematically studying tumor infiltrating immune cells in various malignancies [40]. ssGSEA is a variation of the GSEA algorithm that calculates enrichment scores for groups of samples and sets of genes [41]. Data from Thorsson et al. were used to compare the infiltration of effector cells and natural killer (NK) cells in an ICI cohort. [42] Furthermore, the tumor-infiltrating immune cell subgroups and immune functions between the two groups were quantified using ssGSEA. Potential immune function, immune type, and immune checkpoint signatures were retrieved from recent literature [8,43] and are shown in Table S3.

2.5. Culture conditions

Peripheral blood mononuclear cells (PBMCs) of one healthy donor were isolated via Ficoll-Hypaque density gradient centrifugation using a human peripheral blood lymphocyte isolation kit (Cat# LTS1077, TBD Science, Tianjin, China) according to the manufacturer's instructions. CD8 + T cells were purified from the human PBMCs using an EasySep Human CD8 + T Cell Iso Kit (Cat# 17953, Stemcell Technologies, Vancouver, Canada) according to the manufacturer's instructions. Purified CD8 + T cells were cultured in RPMI-1640 medium (Cat# C11875500BT, Gibco, Thermo Fisher Scientific, Inc) with 10% fetal bovine serum (FBS, Cat# 086–150, Wisent, St-Bruno, QC, Canada), 1% penicillin, and 100 μg/mL streptomycin in 12-well plates (TCP010012, Jet Biofil, Guangzhou Jet Bio-Filtration Co, China), and stimulated for two days with Immunocult Human CD3/CD28 T Cell Activator (Cat# 10971, Stemcell Technologies, Vancouver, Canada) containing recombinant human IL-2 (10 ng/mL) (Cat# 200–02–10, PeproTech, Rocky Hill, NJ, USA). The SK-MEL-246 cell line was cultured in culture plates with DMEM medium (Cat# C11995500BT, Gibco, Thermo Fisher Scientific, Inc), including 10% FBS. For routine cultures, the SK-MEL-246 cells were seeded in 25 cm^2 cell culture bottle (TCF012050, Jet Biofil, Guangzhou Jet Bio-Filtration Co, China). CD8 + T cells were cocultured with tumor cells at a 1:1 ratio in 12-well flat-bottom tissue culture plates and treated with recombinant human IL-21 (Cat# 200–21–2, PeproTech, Rocky Hill, NJ, USA) and/or anti-PD-1 drug (Trepril monoclonal antibody) (Cat# JS001, Shanghai Junshi Biosciences, Shanghai, China) or vehicle. After 48 h of treatment, the cells were harvested from the coculture system, and then flow cytometry was performed.

2.6. Flow cytometry

Single cells were re-suspended in phosphate-buffered saline (PBS, Cat# E607016–0500, Shengong, Shanghai, China) containing 2% FBS and stained with fluorochrome-conjugated or biotinylated antibodies against CD3 (Clone HIT3a, Biolegend, San Diego, CA, USA), CD8 (Clone RPA-T8, BD Biosciences, Franklin Lakes, NJ, USA), and perforin (Clone dG9, Biolegend, San Diego, CA, USA). Dead cells were excluded using Fixable Viability Stain 440UV (Cat# 566332, BD Biosciences, Franklin Lakes, NJ, USA). To detect surface markers, cells were stained with the indicated antibodies for 30 min at 4°C. Before intracellular staining of perforin, cells were stimulated with Cell Stimulation Cocktail plus protein transport inhibitors (Cat# 00–4975–93, eBioscience, San Diego, CA, USA) for six hours. Data acquisition was performed on the CytoFLEX Flow cytometer (Beckman Coulter, Fullerton, CA, USA), and the percentages of cells were calculated using the FlowJo software (FlowJo LLC, Ashland, OR, USA).

2.7. Statistical analysis

Correlations between immune signatures and inflammatory responses were evaluated using Spearman's correlation. The prediction accuracy of the immunotherapy response risk score for CIT was quantified using the area under the curve (AUC), which was calculated using the R software package "ROCR". [44] Univariate and multivariate Cox regression analyses were performed using the Coxph function in R. [45] Survival was estimated according to the Kaplan–Meier method and

compared with the results of the log-rank test. Hazard ratios with 95% confidence intervals (CIs) for 20 cancer types were collected and analyzed using the R package "metafor" based on a random effects meta-analysis model. [46] Statistical significance was defined at a p-value threshold of 0.05. All statistical analyses were carried out using R software version 4.1.0 [47] (https://www.r-project.org/) and GraphPad Prism (GraphPad Software, La Jolla, CA, USA).

3. Results

3.1. Patient characteristics

In this study, we analyzed 12 published datasets that include RNA-seq data of different cancer types, namely, metastatic urothelial cancer, metastatic melanoma, gastric cancer, primary bladder cancer, renal cell carcinoma, and non-small cell lung cancer. The patients were treated with ICI (anti-PD-1/anti-PDL-1/anti-CTLA-4 monotherapy), ACT, MAGE A3 antigen-specific cancer immunotherapy, or BCG immunotherapy. ACT involves the autologous or allogeneic transplantation of tumor-infiltrating lymphocytes or genetically modified T cells expressing novel T-cell receptors or chimeric antigen receptors, and it represents a highly intensive immunotherapy regime that has yielded remarkable response rates in clinical trials of melanoma. [1] MAGE-A3 immunotherapy was designed to enhance humoral and cell-mediated immune responses against MAGE-A3-expressing cells. [2] BCG was initially developed as an agent for vaccination against tuberculosis, and it represents the first successful immunotherapy against established human bladder cancer. [3] CIT response data were available for 784 patients in the 12 datasets and were included in the downstream analysis. A concise description of the 12 datasets is presented in Table S1. After correction, the RNA-Seq data from the 12 datasets were concatenated and randomly partitioned into two subsets, 70% as the training set and 30% as the validation set. In the training cohort, 808 candidate inflammatory response-related genes were extracted based on overlap between a specific GO annotation (GO: 0044546) and GSEA pathway gene (GOBP_INFLAMMATORY_RESPONSE).

3.2. Construction of inflammatory response score

The penalized maximum likelihood estimator was applied to 1000 bootstrap replicates, and 808 candidate inflammatory response-related genes were analyzed using LASSO binomial regression to construct an inflammatory response risk score (Fig. 1A and B). The optimal values of the penalty parameter lambda (Fig. 1B) were determined via 10-fold cross-validation with 1 standard error. Coefficients were obtained to construct a model score composed of eight genes (Fig. 1C).

The inflammatory response-predicting score was developed using a multivariable binary logistic regression model using the following formula:

Inflammatory response score = (0.21491250 ×IL21 mRNA expression value) - (0.03889620 × EXT1 mRNA expression value) - (0.05185152 × ICAM4 mRNA expression value) + (0.17571700 × IFNG mRNA expression value) – (0.03137898 × LPAR1 mRNA expression value)– (0.01954522 × NOX4 mRNA expression value) + (0.02632763 × TAPBP mRNA expression value) + (0.06288640 × TTBK1 mRNA expression value).

3.3. Valuation of the inflammatory response score

A binary classifier was generated using the ROCR package for the high- and low-score groups to determine their potential for differentiating the corresponding responders (R) from the non-responders (NR). The inflammatory response score achieved AUCs of 0.70 (95% CI: 0.59, 0.74), 0.67 (95% CI: 0.59, 0.74), 0.69 (95% CI: 0.66, 0.73) for the training, validation, and overall cohorts, respectively, which suggested a potential role for the inflammatory response score in predicting the response to CIT (Fig. 2A—C).

Next, subjects in the training, validation, and overall cohorts were divided into high- and low-score groups using the optimal cut-off values of the inflammatory response score. The proportion of patients in the high- and low-score groups with 5-year survival was 62% (95% CI: 55, 70%) and 21% (95% CI: 16, 29%; $P < 0{\cdot}001$; Fig. 2D) in the training cohort, respectively; 54% (95% CI: 39, 74%) and 22% (95% CI: 14%, 36%; $P < 0{\cdot}001$; Fig. 2E) in the validation cohort, respectively; and 60% (95% CI: 54%, 67%) and 22% (95% CI: 17%, 28%; $P < 0{\cdot}001$; Fig. 2F) in the overall cohort, respectively. The proportions of patients in the high- and low-score groups with 5-year progression-free survival (PFS) were 47% (95% CI: 27%, 83%) and 15% (95% CI: 19%, 28%; $P < 0{\cdot}001$; Fig. 2G) in the training cohort, respectively; 21% (95% CI: 5%, 94%) and 5% (95% CI: 1%, 3%; $P = 0{\cdot}02$; Fig. 2H) in the validation cohort, respectively; and 52% (95% CI: 30%, 91%) and 5% (95% CI: 4%, 27%; $P < 0{\cdot}001$; Fig. 2I) in the overall cohort, respectively. These results suggested that the inflammatory response score showed a good ability to differentiate patient survival between the high- and low-score groups.

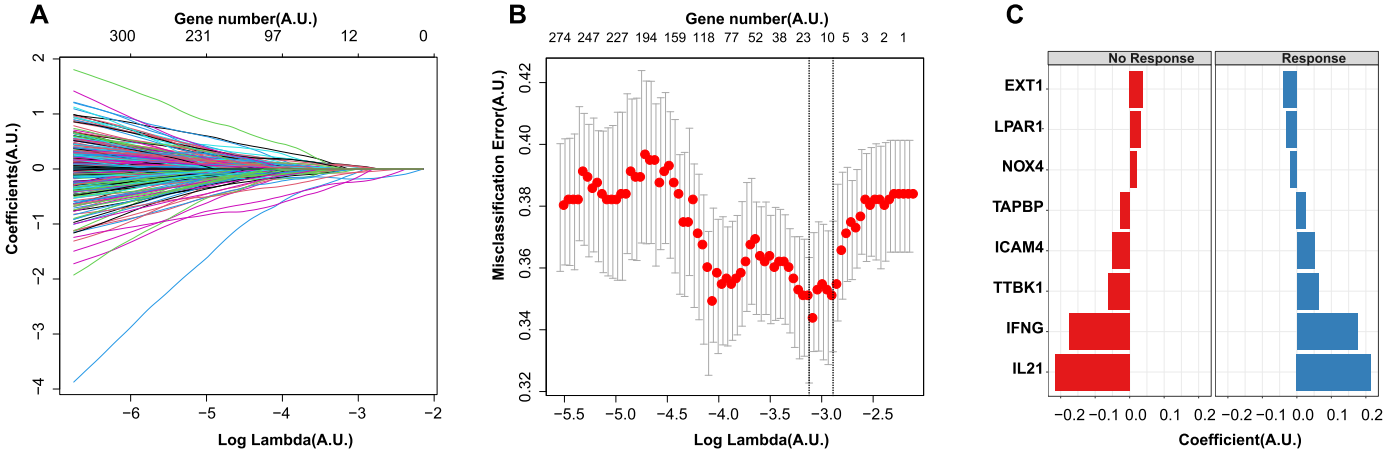

Fig. 1. Constructing an inflammatory response score model for a cancer immunotherapy (CIT) cohort. A. LASSO coefficient profiles of the candidate inflammatory response genes. The horizontal coordinate deviance represents the ratio of the residual explanation, and the ordinate is the coefficient of the gene. B. Partial likelihood deviance of the covariates revealed by the LASSO regression binary model. Points correspond to the means, and error bars correspond to the standard deviations. The numbers above panels A and B represent the number of gene variables involved in the LASSO model. The units of panels A and B are expressed in arbitrary units (A.U.). C. Coefficient values for each of the eight selected genes. A positive weighting coefficient for a gene signature indicates that upregulation of this gene contributes to the probability of a specimen belonging to its type of CIT response. Coefficient values are expressed as arbitrary units (A.U.).

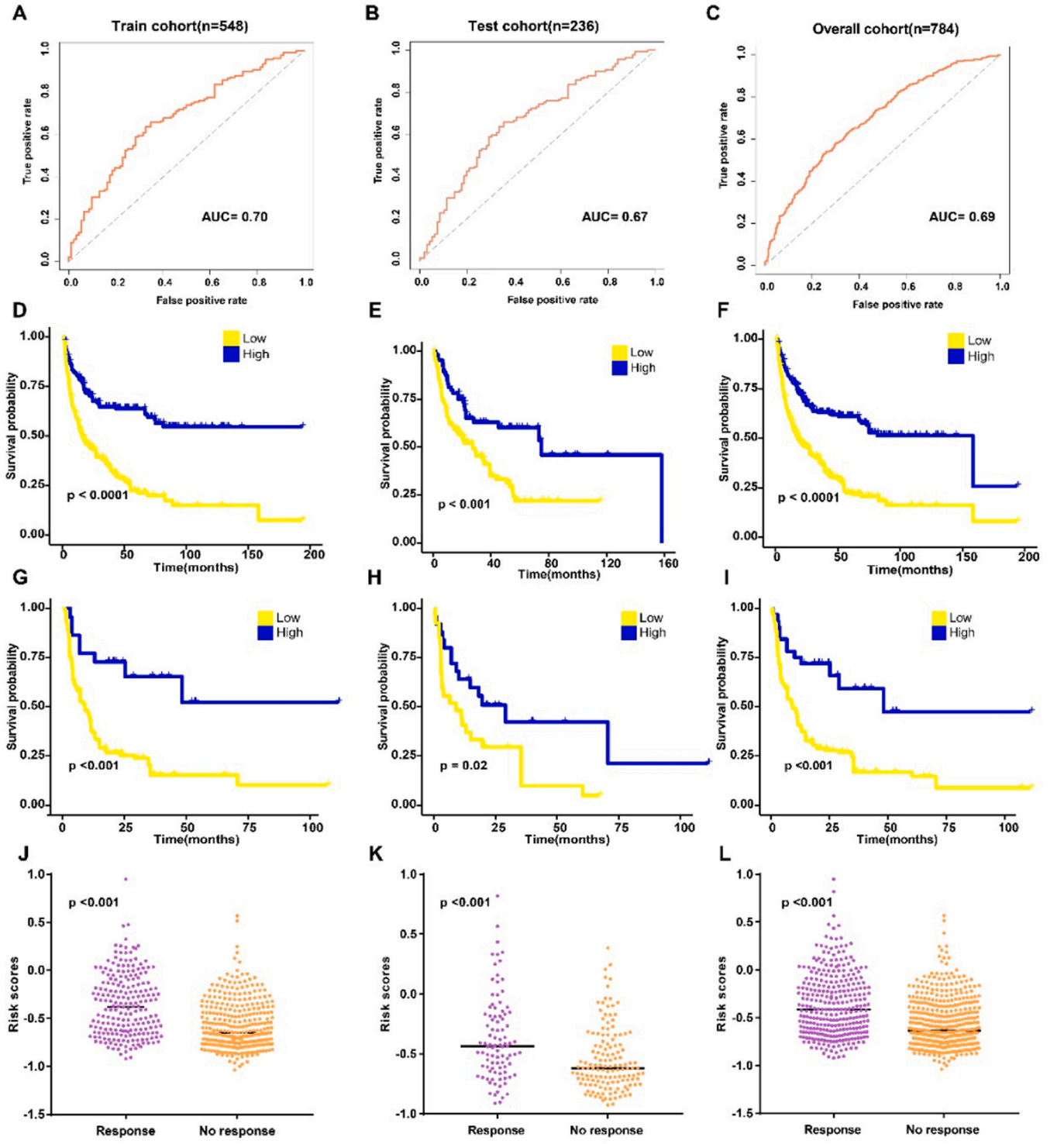

Fig. 2. Validation of the inflammatory response score model. A—C. Assessment of the sensitivity and specificity of the inflammatory response risk score model in each dataset using ROCR analysis. D—I. Kaplan–Meier curves of inflammatory response risk score. Kaplan–Meier curves for overall survival by different immune risk levels in the training (D), validation (E), and overall cohorts (F). Kaplan–Meier curves for progression-free-survival by different immune risk levels in the training (G), validation (H), and overall cohorts (I). J—L. Distribution of the inflammatory response to immunotherapy among samples in the training (J), validation (K), and overall cohorts (L). p values were computed via a one-sided Wilcoxon rank-sum test.

We also observed that the high-score patients had higher response rates (Fig. S2A-C). Subsequently, we found that the inflammatory response scores in patients who responded to immunotherapy were higher than those who showed no response in all three cohorts (Fig. 2J—L). These results also showed that patients in the high-score group were more appropriate for immunotherapy and a higher overall response rate was linked with high inflammatory response scores, which was consistent with the survival analysis findings above.

Analysis of CIT data is complicated by unknown sample purity; thus, several algorithms for estimating sample tumor content based on transcriptomic data have been developed. To address this issue, in the CIT cohort, we used the ESTIMATE algorithm [34] to calculate the tumor

purity in each subject. We then conducted a correlation analysis of the inflammatory response scores and tumor purity and observed a negative correlation between them (Spearman R = −0.47, P < 0.001, Fig. S3A). All patients were divided into low-purity and high-purity tumor groups based on the ESTIMATE score, with the median values as the cut-off: < 0.777 (low purity) and ≥ 0.777 (high purity). Then, using the median inflammatory response score as the boundary, samples were divided into high-score (> −0.560) and low-score groups (< −0.560), and a Kaplan–Meier survival analysis was conducted. The Kaplan–Meier curve analysis showed that the overall OS and PFS of the high-score group were significantly higher than those of the low-score group among the low- and high-purity sets (Fig. S3B and C).

To determine whether the inflammatory response gene signature was an independent prognostic covariate, we tested it via multivariable Cox analyses of the CIT cohort. The inflammatory response score was an independent covariate for OS (Fig. 3A) and PFS (Fig. 3B) in the CIT cohort after adjusting for tumor purity scores. Furthermore, all samples were divided into four groups: group A: ESTIMATE scores > 0.777 and inflammatory response scores > −0.560; group B: ESTIMATE scores > 0.777 and inflammatory response scores < −0.560; group C: ESTIMATE scores < 0.777 and inflammatory response scores > −0.560; and group D: ESTIMATE scores < 0.777 and inflammatory response scores < −0.560. Log-rank tests demonstrated significant differences in the distribution of both OS (Fig. 3C) and PFS (Fig. 3D). Group A experienced a longer OS period than the other three groups (Fig. 3C). Although PFS did not significantly differ between Group A and the other three groups, a trend of longer PFS was observed in patients with high inflammatory response scores (Fig. 3D).

Previous studies [10,11,21,48] have revealed that predictive signatures derived from on-treatment samples of metastatic melanoma are superior to those derived from pre-treatment samples in terms of predicting ICB response. This indicates that the signatures in patients prior to and during ICB immunotherapy should be identified and evaluated.

The sensitivity and specificity of the inflammatory response score between on- and pre-treatment metastatic melanoma tumor tissues were assessed using receiver operating characteristic (ROC) analysis. Since all on-treatment samples (n = 84) are treated with ICB therapy, we only performed the ROC analysis in 264 pre-treatment metastatic melanoma patients treated with ICB therapy. We found that the inflammatory response scores derived from the on-treatment tumor specimens had a higher AUC (0.80; 95% CI: 0.67, 0.93; Fig. 4A) than that those derived from the pre-treatment samples (0.66; 95% CI, 0.59, 0.72; Fig. 4B). The Kaplan–Meier cumulative curve indicated that patients with high scores survived significantly longer than those with low scores. The proportions of patients with 5-year survival in the high- and low-score groups were 90% (95% CI: 73%, 100%) and 35% (95% CI: 24%, 51%; $P < 0{\cdot}001$; Fig. 4C) in the on-treatment cohort, respectively; 69% (95% CI: 60%, 80%) and 33% (95% CI: 25%, 44%; $P < 0{\cdot}001$; Fig. 4D) in the pre-treatment cohort, respectively. The proportions of patients with 5-year PFS in the high- and low-score groups were 57% (95% CI: 24%, 100%) and 8% (95% CI: 3%, 23%; $P < 0{\cdot}001$; Fig. 4E) in the on-treatment cohort, respectively; and 46% (95% CI: 33%, 65%) and 14% (95% CI: 6%, 31%; $P < 0{\cdot}001$; Fig. 4F) in the pre-treatment cohort, respectively.

Considering that the clinical characteristics of most of the patients in the CIT cohort were incomplete, a sub-group of 235 patients with metastatic urothelial cancer with complete clinical information was constructed. The AUC for predicting the response to CIT in patients with metastatic urothelial cancer according to the risk score was 0.71 (95% CI: 0.64, 0.78; Fig. S4A). Patients with high scores showed greater OS than those with low scores, and their 2-year survival rate was 63% (95% CI: 50%, 80%) and 27% (95% CI: 51%, 92%; $P < 0.001$, Fig. S4B), respectively. Multivariable Cox regression analyses showed that the inflammatory response score was independently correlated with survival, with a HR of 0.27 (95% CI: 0.14, 0.51; $P < 0.001$; Fig. S4C) in the metastatic urothelial cancer dataset.

The CIT response is related to various treatment modalities in different entities. We further performed ROC analyses of the different cancer types and obtained AUCs of 0.82, 0.80, 0.71, 0.70, 0.67, and 0.64 for the non-small cell lung cancer, gastric cancer, metastatic urothelial cancer, primary bladder cancer, metastatic melanoma, and renal cell carcinoma cohorts, respectively (Fig. S5A). The small sample size in the

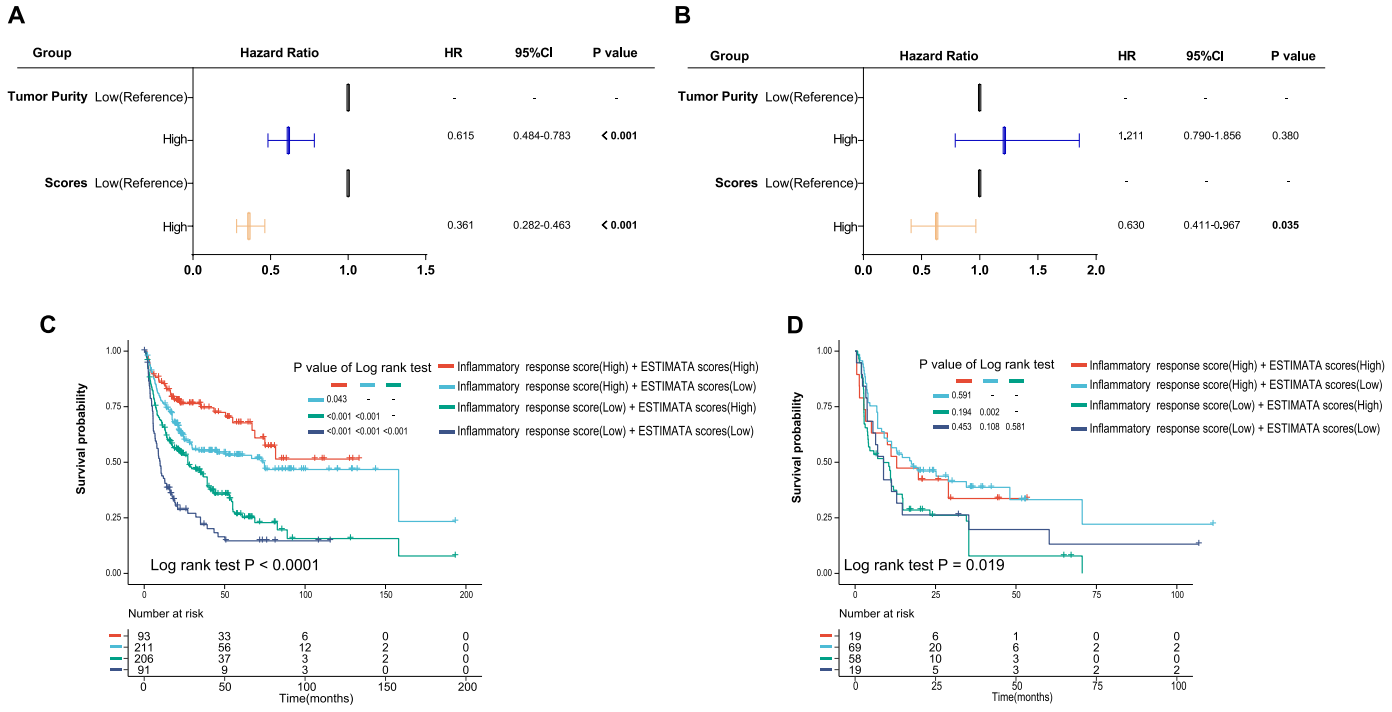

Fig. 3. Identification of inflammatory response score model associated with patient survival. A-B. Multivariate regression analysis of OS (A) and PFS (B) in patients from CIT cohorts. C-D. OS (C) and PFS (D) analysis among four groups stratified by both ESTIMATE scores and inflammatory response. P-values less than 0.05 are in bold in the figure.

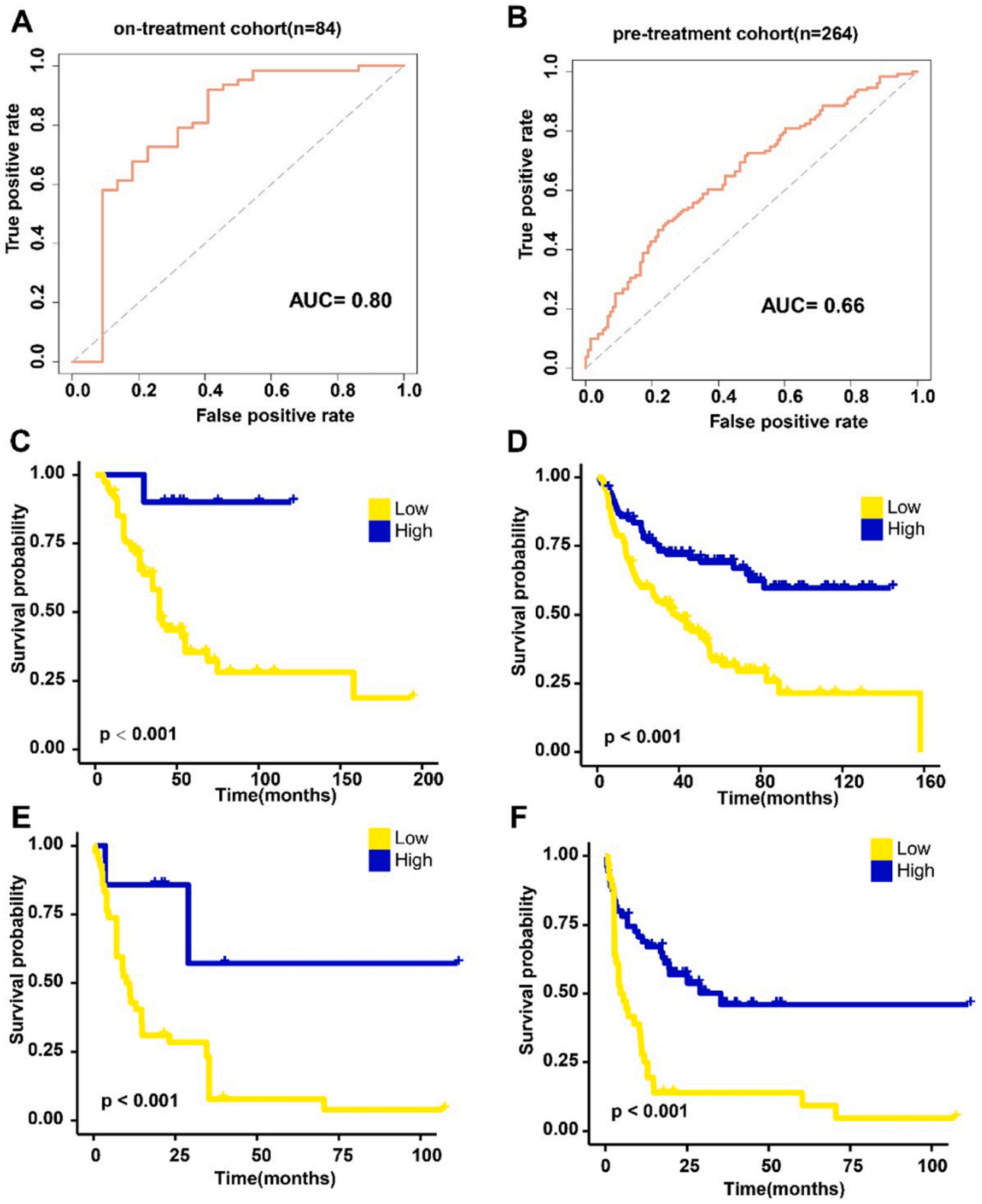

Fig. 4. Evaluation of the inflammatory response score in tumor species of on-treatment and pre-treatment patients with metastatic melanoma. A—B. Receiver operating characteristic curves of inflammatory response risk score in predicting immunotherapy response between on-treatment and pre-treatment cohorts of patients with metastatic melanoma. C—D. Kaplan–Meier curves of inflammatory response score for overall survival by different inflammatory response score levels in the on-treatment (C) and pre-treatment cohort (D). E—F. Kaplan–Meier curves of inflammatory response score for progression-free survival by different inflammatory response score levels in the on-treatment (E) and pre-treatment cohort (F).

renal cell carcinoma cohort (n = 11) led to high uncertainty in model development, which limited the predictive performance of the model. In response to CIT, cells within the tumor microenvironment may undergo significant alterations at the transcriptome level. Tumor tissues collected before and after treatment may show a high degree of heterogeneity and thus could obtain a low AUC value for the metastatic melanoma cohorts.

Two out of eight genes (IL21 and IFNG) included in the inflammatory response score presented substantially higher coefficients in the final model (Fig. 1C), meaning that they outweigh the overall score value. This is in line with previous reports on the predictive significance of tumor expression of IL21 [49] and IFNG [9]. An analysis of the predictive performance of the signatures of the two genes (IL21 +IFNG) revealed that the ROCs of the training and test cohorts were 0.65 and 0.67, respectively (Fig. S5A and B). Although the accuracy of the eight genes is indeed slightly improved, an assay based on the score of the two genes (IL21 +IFNG) may have greater potential for use in treatment monitoring because it is superior in terms of both financial and technical handiness.

3.4. Association between inflammatory response score and immunity in the CIT cohort

To assess the relationship between inflammatory response scores and immune responses in patients with cancer receiving CIT, we compared the ESTIMATE [34], EPIC [50], MCPcounter [36], Immune AI [37], CIBERSORT [38], Xcell [39], and ssGSEA [41] algorithms and estimated the changes of immune cell types and functions between the high- and low-score groups based on inflammatory response gene signatures in the overall CIT cohort (Fig. 5A, Table S4). Correlation analysis revealed that the infiltration of effector and NK cells and immune functions, including checkpoint molecules, co-stimulatory ligands, co-stimulatory receptors, cytolytic (CYT) activity, interferon (IFN) response, MHC-I, MHC-II, T helper 1 cell (Th1), T helper 2 cell (Th2), and tumor-infiltrating lymphocyte (TIL) signatures was significantly higher in the high-score group than in the low-score group (Fig. 5B, Table S5). We also observed that the higher the model score, the higher proportion of immune cell infiltration, including B cells, effector cells, and NK cells (Fig. 5C).

In addition, we further investigated the differences in the expression of eight immune checkpoints between the high- and low-score groups. Patients with higher HAVCR2, TIGIT, BTLA, CD274, CTLA4, LAG3, PDCD1, and PDCD1LG2 levels presented a higher inflammatory response score (Fig. 5D—K, Table S6).

3.5. Comparison of inflammatory response signatures and published predictive signatures

We then evaluated the predictive performance of the inflammatory response signatures derived from on-treatment specimens. To this end, we further compared the inflammatory response scores against those of previously reported transcriptome-based predictive signatures, including the epithelial-to-mesenchymal transition (EMT). Sig [51], immuno-predictive score (IMPRES). Sig [52], innate anti-PD-1 resistance (IPRES). Sig [53], LRRC15 + carcinoma-associated fibroblasts (LRRC15. CAF). Sig [54], immune-related genes (IRG). Sig [55], anti-CTLA4 resistance MAGE gene (CRAM). Sig [56], PDL1. Sig [57], plasma.cells.Sig [58], cytolytic activity (CYT). Sig [59], and CD8. Sig [57]. This analysis indicated that the inflammatory response signature derived from on-treatment specimens was the most effective at predicting the responses to ICB therapy (Fig. 6, Table S7).

3.6. Pan-cancer profiling of inflammatory response scores

To explore the pan-cancer distribution characteristics of the inflammatory response scores, we analyzed approximately 7000 tumors of 20 cancer types from TCGA. These 20 cancers showed significant differences in the inflammatory response scores (analysis of variance, $P < 0{\cdot}0001$, Fig. 7A, Table S8), indicating a distinctive intensity of inflammation with diverse cancers. Lung adenocarcinoma (LUAD) and ovarian serous cystadenocarcinoma (OV) had the highest and lowest average inflammatory response scores, respectively.

Univariate Cox regression analyses for the TCGA cohort suggested that the inflammatory response risk score was associated with a good prognosis in a wide array of tumor types, including BRCA, BLCA, CESC, GBM, THCA, HNSC, SKCM, and LUAD. In a meta-analysis, the inflammatory response risk score tended to be associated with a good prognosis in terms of OS (Fig. 7B, Table S9). The proportion of cancer cells in a tumor sample is called the tumor purity, and it represents an important factor to consider in genomic analyses of bulk tumors. TCGA analyses are complicated with unknown tumor purity, and consensus measurement of purity estimation (CPE) [60] algorithms for estimating sample tumor content based on transcriptomic data have been developed to address this issue. Patients in the TCGA cohort were divided into three groups based on their CPE scores using the following cut offs: < 0.6 (low-purity group), 0.6–0.9 (medium-purity group), and ≥ 0.9 (high--purity group). For each group, a meta-analysis analysis was conducted on subgroups to determine their survival. We found that the inflammatory response score tended to be associated with a longer OS in the low-purity group and medium-purity group but not in the high-purity group (Fig. S6). These results revealed that the predictive performance of inflammatory response scores in patients who had not undergone immunotherapy could be affected by the purity of the tumor.

3.7. Inflammatory response score is significantly correlated with immunity in 20 cancer types

To elucidate the association between the inflammatory response risk score and tumor immunity, GSEA was performed. This analysis indicated significant enrichment of genes involved in immune-related pathways in hallmark gene sets, particularly the interferon alpha/gamma response pathways, in all 20 cancer types with high inflammatory response scores. This suggests that a high inflammatory response score is markedly associated with the interferon alpha response and interferon gamma response signaling pathways (Fig. 8A, Table S10). These findings were further validated using Reactome gene sets (Fig. S7, Table S11).

Furthermore, we examined diverse immune signatures, including checkpoint molecule, co-stimulatory ligand, co-stimulatory receptor, immune CYT, IFN response, MHC-I gene, MHC-II gene, and TIL infiltration signatures. Each immune signature includes several representative gene markers (Table S3). The CYT scores were defined by granzyme A and perforin expression, which are dramatically reflected the activation of CD8 + T cell and immune status [34]. IFNs can modulate innate immune responses in a balanced manner that promotes antigen presentation and NK cell functions [34]. The MHC is a group of genes that encode proteins on the cell surface that have an important role in immune response. Their main role is to bind peptide fragments derived from genomic mutations or pathogens and display them on the cell surface for recognition by cognate T cells to initiate an immune response. [61] TILs are a mixture of proinflammatory immune cells in the tumor microenvironment, including cytotoxic T cells, helper T cells, regulatory T cells, and B cells. They can influence the prognosis of cancer patients by directly or indirectly participating in immune responses [8]. Strikingly, we found that the inflammatory response score was highly correlated with the CYT and TIL immune signatures in the 20 cancers (Fig. 8B, Table S12). Given the high degree of correlation between the immune response score and CYT among these five immune signatures, we performed a marker gene expression analysis based on a ssGSEA, the TIMER database, and data from Thorsson et al. to further illustrate the relationships between the score and effector cells and NK cells. These cells mainly secrete GZMA and PRF1, which represent an indicator of CYT in tumors. We obtained consistent results from the ssGSEA

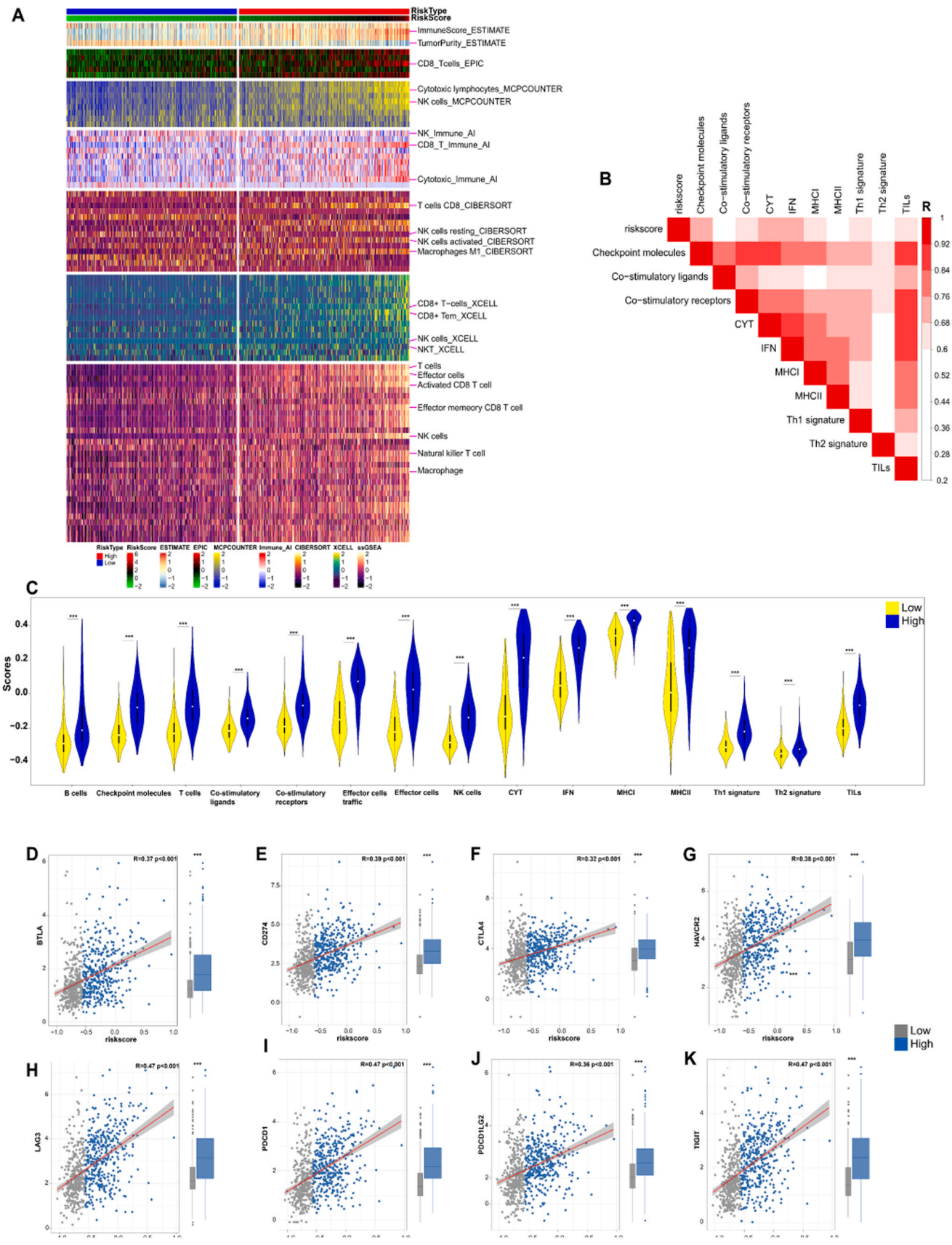

Fig. 5. Validation of the inflammatory response score model. A. Heatmap for immune responses based on the ESTIMATE, EPIC, MCPcounter, Immune AI, CIBERSORT, Xcell, and single-sample gene set enrichment analysis (ssGSEA) algorithms among high and low score groups. B. Correlation matrix heat map showing the relationship between inflammatory response risk scores and expression levels of immune cell and immune signatures in the cancer immunotherapy cohort. R: Spearman's correlation coefficient. C. Expression of immune cell and immune signature between high- and low inflammatory response score groups.

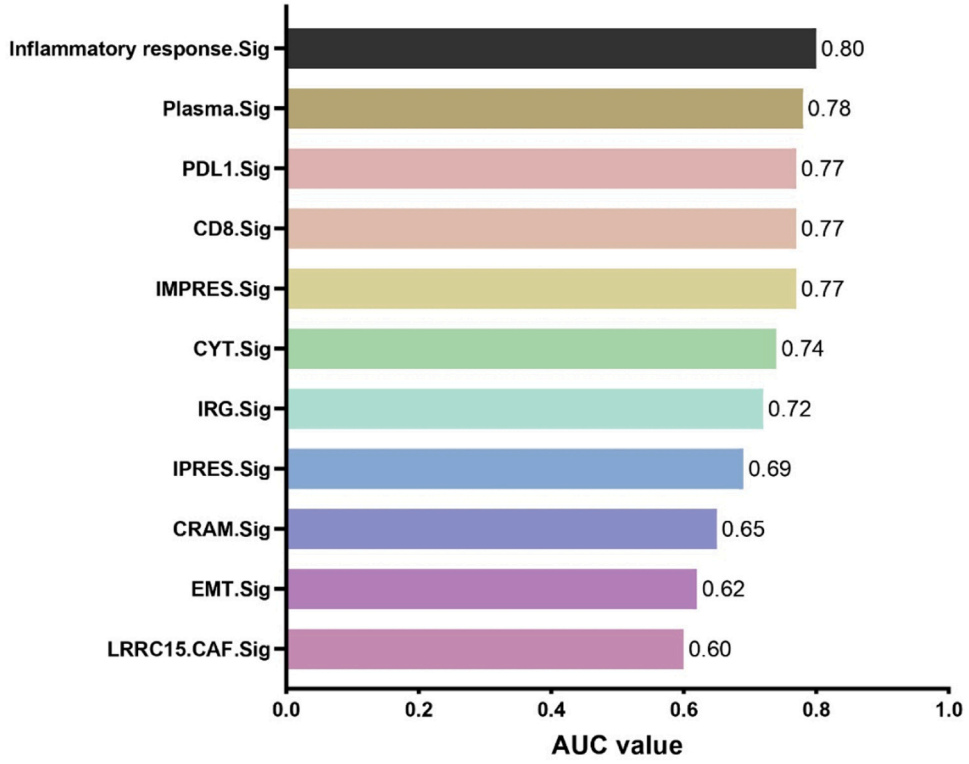

Fig. 6. Comparison of predictive performance of inflammatory response gene signature against other CIT response signatures. Bar plots of AUCs for 11 CIT response signatures are shown for the on-treatment cohorts. Each cohort's sample number is shown in the legend.

(Fig. 8C—D), TIMER database (Fig. 8E—-F), and Thorsson et al. data (Fig. 8G—H), which showed that LUAD, LUSC, UCEC, BLCA, CESC, LIHC, BRCA, COAD, SKCM, KIRC, THCA, and HNSC (Table S12) displayed higher levels of effector cells and NK cell infiltration in the high-score group compared with the low-score group (Mann–Whitney U test, $P < 0{\cdot}05$ for all cases). This suggested that the inflammatory response signature score may influence tumor immunity mainly by mediating the CYT of immune cells, which is consistent with the tumor immunity analysis in the CIT cohort.

Significant associations between the inflammatory response score and immune checkpoints at the individual level across the 20 cancer types were observed (Fig. 8H). Subsequently, estimation of the immune checkpoint levels revealed that 17 cancer types (BLCA, BRCA, CESC, COAD, ESCA, GBM, HNSC, KIRC, LIHC, LUAD, LUSC, OV, READ, SKCM, STAD, THCA, and UCEC) demonstrated a significant increase in checkpoint molecule scores in the high-score group compared with the low-score groups, whereas three cancer types (KIRP, PAAD, and PRAD) did not (Fig. 8J).

3.8. IL21 significantly increased the cytotoxicity of CD8 + T cells

Using the inflammatory response score model, the score with the highest weight was assigned to IL21. To determine whether IL-21 promoted the cytotoxicity of CD8 + T cells co-cultured with melanoma cells, CD8 + T cells/SK-MEL-246 cells were co-cultured alone in 12-well plates in normal medium or medium treated with IL-21 (human recombinant IL-21) and/or anti-PD1 monoclonal antibody (Trepril monoclonal antibodies). Flow cytometry revealed that the cytotoxic activity of CD8 + T cells was improved after treatment with IL-21 + anti-PD1 monoclonal antibody (Fig. 9**A** and **B**).

4. Discussion

Cancer immunotherapy (CIT) has revolutionized the treatment of multiple types of tumors [62], although only a subset of patients has shown profound clinical benefits and durable responses [63]. To optimize therapeutic decision-making, robust and concise features that predict CIT treatment response must be identified.

Inflammation of the tumor microenvironment is an important event that impacts the therapeutic response and survival. In this study, we evaluated the potential response to CIT therapy by building a concise yet effective predictive model based on only eight inflammatory response genes. Our study demonstrated that inflammatory response gene scores are effective biomarkers of CIT responses. Regardless of the tumor purity, patients in the low-score group had a significantly poorer prognosis than those in the high-score group. Previous studies have pointed out that a high-inflammation tumor microenvironment contains an abundance of proinflammatory cytokines, such as IL-1β, IL-12 and IL-2, which contribute to T-cell activation and expansion. [12] The results of the immunity analysis in the CIT cohort revealed that TILs, including B cells, effector T-cells, M1 macrophage cells, and Th1 cells, were significantly increased in the high score group, and that some immune-activated functions (i.e., T-cell co-stimulation, MHC-mediated antigen presentation, and CYT activity) were significantly enriched in the high-score group compared with the low-score group. This might explain why patients with high inflammatory response scores had a higher rate of response to CIT, their trend towards longer OS, and significantly better PFS compared with those patients with low scores.

Previous studies have suggested that on-treatment tumor samples can more reliably predict patients' endocrine therapy responses compared to pre-treatment samples in breast cancer [64,65]. However, gene signatures capable of predicting response to CIT therapies in melanoma have largely been identified based on the association between pre-treatment samples and patients' clinical response. We assessed the performance of inflammatory response gene signatures in predicting the responses of melanoma to ICB therapy and found that the AUC for the inflammatory response gene signatures derived from the on-treatment samples was 0.80, which was more informative than the AUC for the

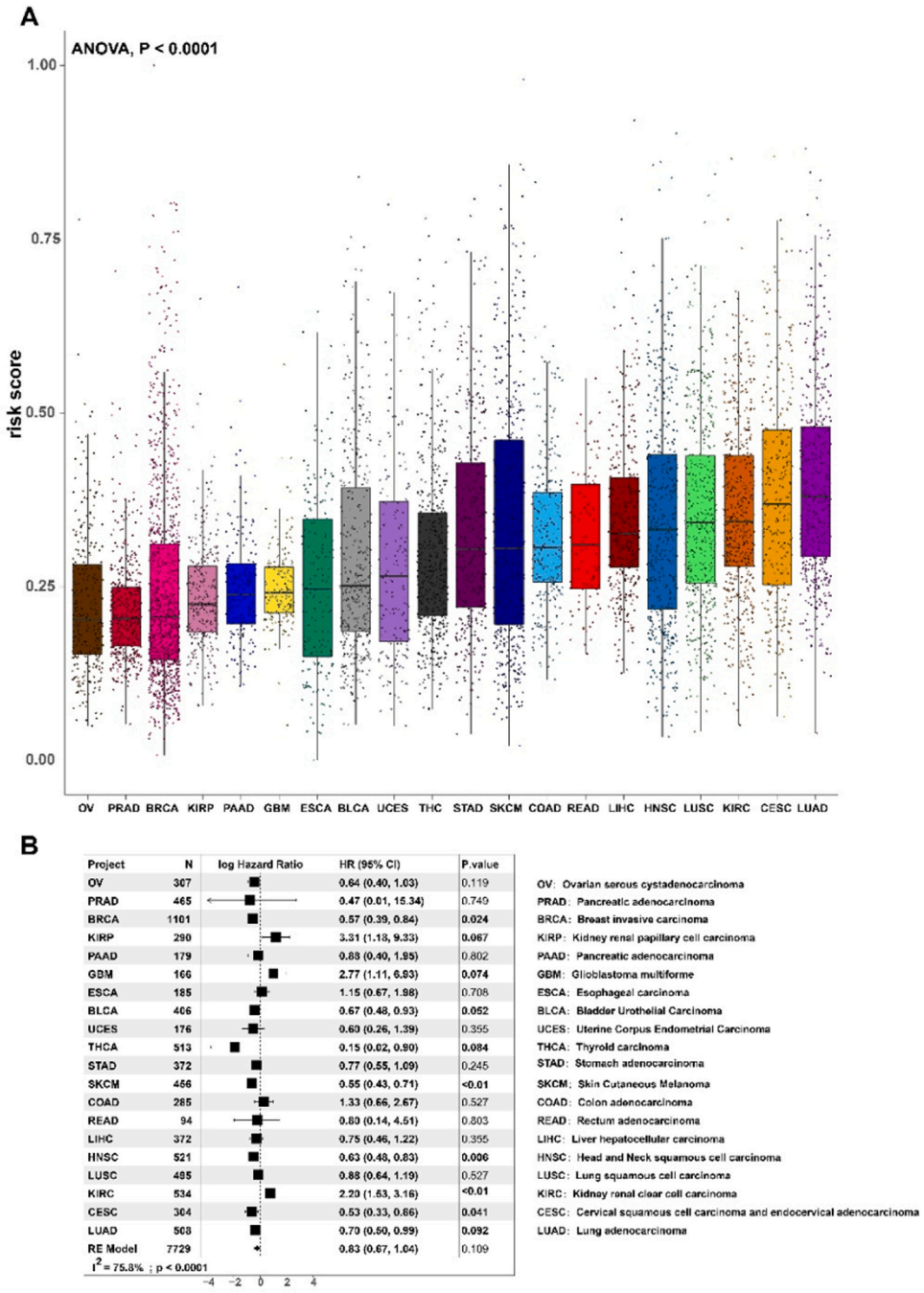

Fig. 7. Inflammatory response score analysis in 20 cancer types. A. Inflammatory response risk scores among all samples grouped by cancer. Risk scores of each patient are measured on a scale of 0–1. B. Results of the Cox proportional hazards regression of the OS analysis using inflammatory response risk scores for 20 cancer types. If the p-value is less than 0.05, it is shown in bold font. A random-effects meta-analysis was used to generate the pooled hazard ratios and p-values. Statistical test of heterogeneity is shown in the last column.

inflammatory response gene signatures derived from the pre-treatment samples. Our results demonstrated that the inflammatory response gene signature scores for on-treatment samples are more robust predictors of the response to ICB in metastatic melanoma. As cancer therapies generally induce complicated changes in genes, it makes sense that on-treatment samples may provide more valuable insights into the dynamic changes at the transcriptional level correlated with clinical response. These findings have implications for treatment selection in current clinical practice because most studies have used pretreatment biopsies to construct prediction signature. Accurate on-treatment signatures scores can help medical oncologists identify subgroup of patients who will more likely benefit from CIT therapies. Inflammatory response gene signatures from on-treatment samples can be used to identify patients who will not benefit from CIT treatment immediately after treatment initiation before substantial toxicities and costs are incurred.

Furthermore, we defined the inflammatory response score spectrum of over 7000 tumor samples from 20 cancer types. Owing to the tissue-specific/cell-specific role of inflammatory response intensity, there are discrepancies in the inflammatory response scores in diverse cancers. The inflammatory response score was significantly associated with OS in BRCA, KIRP, GBM, BLCA, THCA, SKCM, HNSC, KIRC, LUAD, and CESC,

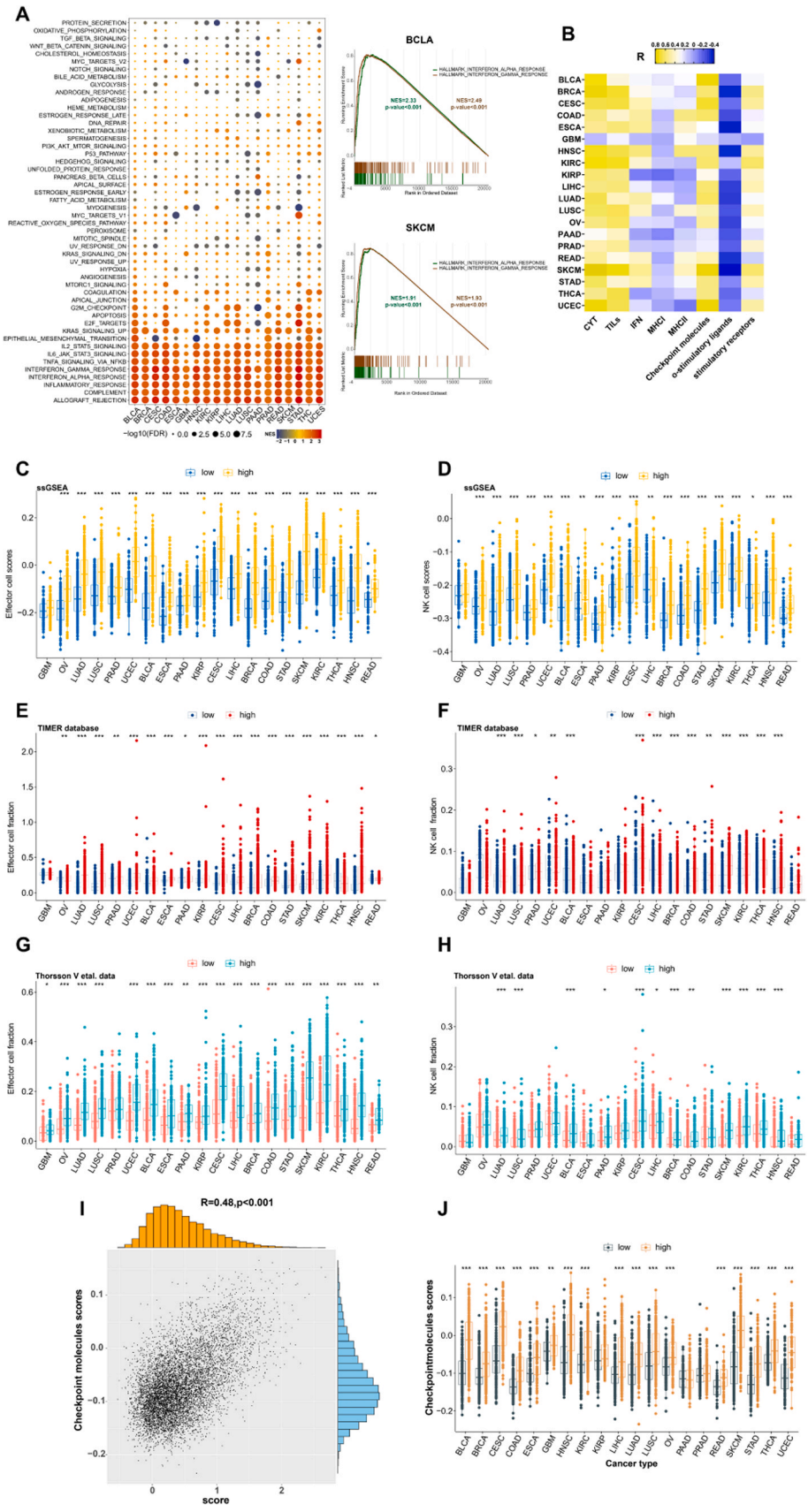

(caption on next page)

Fig. 8. Relationships between inflammatory response scores and signaling pathways and immunophenotypes. A. Relationships between inflammatory response risk scores and signaling pathways in patients with cancer with high and low scores. Normalized enrichment scores (NES) and p-values were determined using the GSEA algorithm. B. Correlation of inflammatory response scores with diverse immune signatures including CYT, TILs, IFN, MHCI, and MHCII in 20 cancer types from The Cancer Genome Atlas (TCGA). R: Spearman's correlation coefficient. D—I. The infiltration levels of effector cells and natural killer (NK) cells in the low and high score groups were stratified by the inflammatory response risk scores in 20 cancer types from TCGA using marker gene expression analysis (D—E), the TIMER database (F—G), and the data of Thorsson et al. (H—I). P values were calculated on the Mann–Whitney test. J: Correlation between checkpoint molecule scores and inflammatory response scores in 7729 cancer samples. R: Spearman's correlation coefficient. J: The checkpoint molecule scores in low and high risk score groups stratified by the inflammatory response risk scores in 20 cancer types. P values were calculated on the Mann–Whitney test.

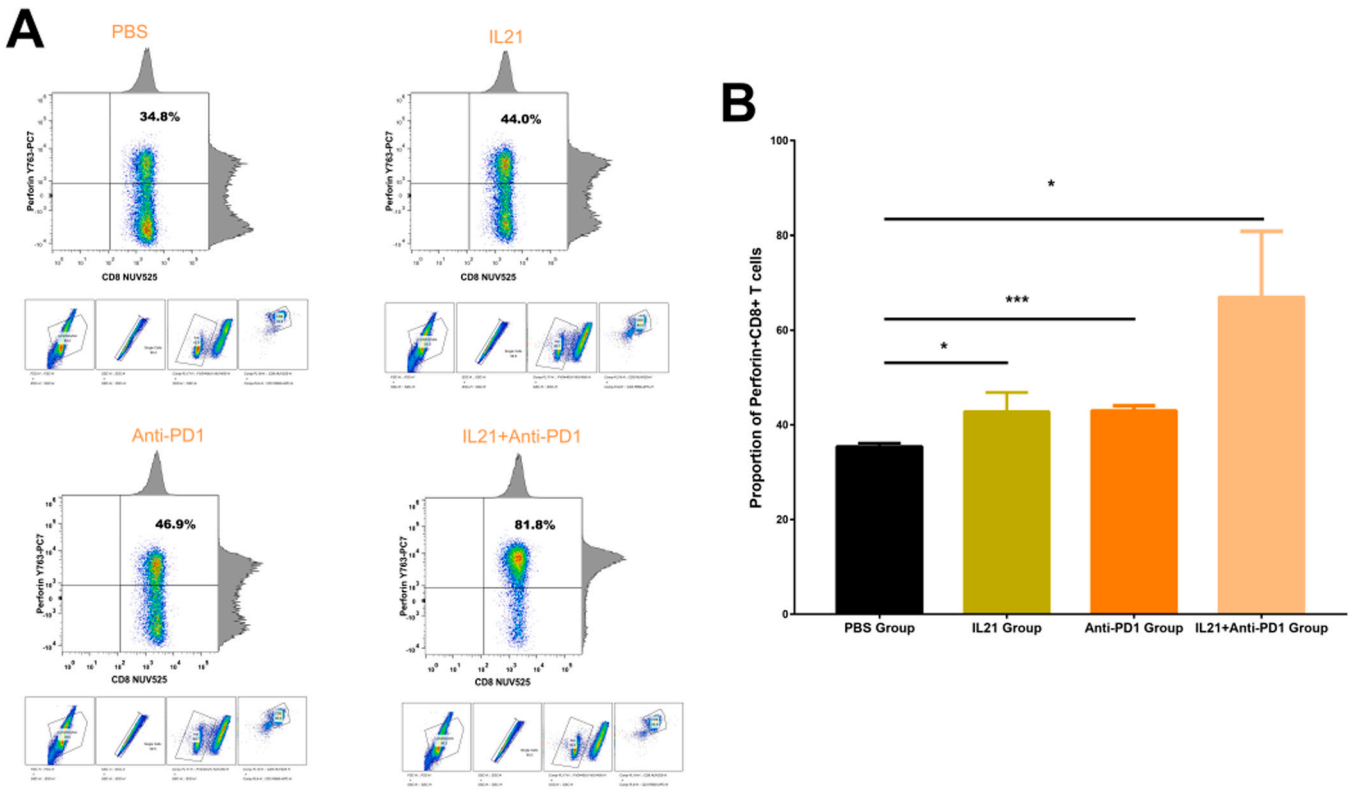

Fig. 9. Frequency of perforin+CD8 + T cells is increased in CD8 T cells/SK-MEL-246 cells treated with IL21 plus Anti-PD1 monoclonal antibody. Representative FlowJo smoothing coexpression of CD8 with perforin (A). Data are represented as box and bar graphic plots (B), and error bars represent the mean and SD (n = 3). P values were calculated based on a Student test.

and similar immunity analysis results were obtained for the TCGA cancer type cohort. However, the prognostic performance of inflammatory response scores in TCGA cancer patients can be affected by tumor purity, which was inconsistent with above results found for the CIT cohort. These findings indicated that researchers need to be cautious when using inflammatory response scores to predict survival of cancer patients who have not received immunotherapy.

The expression levels of immune checkpoint genes, such as those encoding PD-1, PDL-1, and CTLA-4, have been explored as biomarkers for the prediction of the CIT response. [66] The inflamed-tumor immune microenvironment is characterized by high infiltration of cytotoxic T lymphocytes (CTLs) expressing PD-1 and tumor cells expressing PDL-1 [67]. In our study, a significant association between inflammatory response scores and immune checkpoint gene levels was found in both the CIT cohort and all 20 TCGA cancer types, indicating that patients in the high-score group were more likely to have an infiltrated-inflamed tumor microenvironment. This indicated that patients with cancer in the inflammatory response low-score group received local application of inflammatory signals to amplify the pro-inflammatory signals and promote immune cell recruitment, whereas those with high scores also encountered a blockade of immune inhibitory pathways mediated by immune checkpoints.

IL21 showed the highest prognostic significance in patients with cancer undergoing CIT. Previous studies have demonstrated the antitumor effects of IL21 in the immune microenvironment. For example, IL21 exerts antitumor effects by enhancing the cytotoxicity of CD8 + T-cells and NK cells. [68,69] IL21 therapy combined with checkpoint blockades enhances the antitumor effect by inducing NK cells to tumor sites and reducing the frequency of dysfunctional tumor antigen-specific CD8 + T-cells inside the tumor microenvironment. [70,71] In our study, we reported similar results and showed that the cytotoxic activity of CD8 T-cells was increased when using IL21 + anti-PD1 antibody treatment in CD8 T cells/SK-MEL-246 cells compared to that of the PBS group. The high-score group with an immune activation environment expressed high levels of checkpoint molecules, probably due to the high expression levels of IL21.

This study has several limitations. First, the prediction response rate needs to be improved further. The AUC was approximately 0.7 in the training cohort and 0.67 in the test cohort. In the CIT cohort, the inflammatory response scores had relatively higher AUC values for the response for non-small cell lung cancer and gastric cancer but lower AUC values for renal cell carcinoma. Thus, inflammatory response scores exhibited varying predictive implications in different tumor types because of tumor heterogeneity. The inflammatory response score appears represent an appropriate initial estimate of inflammatory responses in cancers and should not be considered a prediction. Second,

owing to dataset access limitations, the RNA-Seq data for approximately 700 patients were obtained and analyzed in the study. However, a higher number of patients are required to verify the immunotherapy response model in the future. Third, it is impossible to evaluate whether the model can serve as an independent prognostic factor for bladder cancer or other cancer types due to a lack of complete clinical variables. Finally, the detailed mechanism underlying the impact of most model genes on the response to immunotherapy is unclear. Therefore, this issue is worthy of further study.

In conclusion, we developed and validated an immunotherapy response prediction model for multiple cancers that involves the expression of inflammatory response genes. Inflammatory response score signatures derived from on-treatment samples have a high ability to predict the efficacy of CIT response in patients with metastatic melanoma. Our data also suggest that inflammatory response genes can serve as independent prognostic factors in BLCA under CIT conditions. Further immunity analyses indicated that inflammatory response gene signatures may influence tumor immunity, mainly by mediating CYT and TILs, particularly effector cells and NK cells. Our study highlighted the impact of the inflammatory response scores on the immunotherapy response. These findings can pave the way for further investigations on the prognostic and therapeutic potential of inflammatory response scores. Moreover, an inflammatory response model should be developed as a new approach for predicting patient survival and response to cancer immunotherapy.

Ethics approval

All procedures performed in studies involving human subjects were approved by the ethics committee of Sun Yat-sen University Cancer Center and were in accordance with the 1964 Declaration of Helsinki and its later amendments or comparable ethical standards. Informed consent was obtained from all participants included in the study.

Funding

Y.L. is supported Sun Yat-sen University Start-up Funding (Grant No. 201603). Y.W. is supported by the National Natural Science Foundation of China (Grant No. 82100184), the Natural Science Foundation of Guangdong (Grant No. 2022A1515012521), the Beijing Xisike Clinical Oncology Research Foundation (Grant No. Y-Young2022-0281), and the Science and Technology Planning Project of Guangzhou (Grant No. 202201010919). S.C. is supported by National Funded Postdoctoral Program of China (Grant No. GZC20231518).

CRediT authorship contribution statement

S.C. and M.H. performed the research and collected the data. S.C. and L.Z. carried out the flow cytometric analysis. S.C., M.H., L.Z., and Q.H. wrote the manuscript. Y.W. and Y.L. designed this study, and reviewed and edited the manuscript. All of the authors gave their final approval of the version submitted for publication.

Declaration of Competing Interest

The authors declare that they have no known competing financial interests or personal relationships that could have appeared to influence the work reported in this paper.

Acknowledgments

We thank Jianming Zeng (University of Macau) and all the members of his bioinformatics team and biotrainee for generously sharing their experiences and codes. We thank Editage (https://www.editage.cn/) for English language editing. We thank Ms. Chunjie Wu for providing some valuable opinions and suggestions on our works.

Appendix A. Supporting information

Supplementary data associated with this article can be found in the online version at doi:10.1016/j.csbj.2023.12.001.

References

[1] Lauss M, et al. Mutational and putative neoantigen load predict clinical benefit of adoptive T cell therapy in melanoma. Nat Commun 2017;8. https://doi.org/10.1038/s41467-017-01460-0.
[2] Ulloa-Montoya F, et al. Predictive gene signature in MAGE-A3 antigen-specific cancer immunotherapy. J Clin Oncol 2013;31. https://doi.org/10.1200/JCO.2012.44.3762.
[3] Kim Y-J, et al. Gene signatures for the prediction of response to bacillus calmette-guerin immunotherapy in primary pT1 bladder cancers. Clin Cancer Res: J Am Assoc Cancer Res 2010;16:2131–7. https://doi.org/10.1158/1078-0432.CCR-09-3323.
[4] Robert C. A decade of immune-checkpoint inhibitors in cancer therapy. Nat Commun 2020;11:3801. https://doi.org/10.1038/s41467-020-17670-y.
[5] Xiong D, Wang Y, You M. A gene expression signature of TREM2 macrophages and γδ T cells predicts immunotherapy response. Nat Commun 2020;11. https://doi.org/10.1038/s41467-020-18546-x.
[6] Rodig S, et al. MHC proteins confer differential sensitivity to CTLA-4 and PD-1 blockade in untreated metastatic melanoma. Sci Transl Med 2018;10:eaar3342. https://doi.org/10.1126/scitranslmed.aar3342.
[7] Johnson D, et al. Melanoma-specific MHC-II expression represents a tumour-autonomous phenotype and predicts response to anti-PD-1/PD-L1 therapy. Nat Commun 2016;7:10582. https://doi.org/10.1038/ncomms10582.
[8] Ju M, et al. Pan-cancer analysis of NLRP3 inflammasome with potential implications in prognosis and immunotherapy in human cancer. Brief Bioinforma 2020;22. https://doi.org/10.1093/bib/bbaa345.
[9] Ayers M, et al. IFN-γ–related mRNA profile predicts clinical response to PD-1 blockade. J Clin Investig 2017;127. https://doi.org/10.1172/JCI91190.
[10] Chen S, et al. Comprehensive analysis of glycoprotein VI-mediated platelet activation signaling pathway for predicting pan-cancer survival and response to anti-PD-1 immunotherapy. Comput Struct Biotechnol J 2023;21:2873–83. https://doi.org/10.1016/j.csbj.2023.04.002.
[11] Chen S, Zhang L, Lin H, Liang Y, Wang Y. Functional gene expression signatures from on-treatment tumor specimens predict anti-PD1 blockade response in metastatic melanoma. Biomolecules 2022;13. https://doi.org/10.3390/biom13010058.
[12] Chen D, Mellman I. Elements of cancer immunity and the cancer–immune set point. Nature 2017;541:321–30. https://doi.org/10.1038/nature21349.
[13] Harlin H, et al. Chemokine expression in melanoma metastases associated with CD8(+) T-cell recruitment. Cancer Res 2009;69:3077–85. https://doi.org/10.1158/0008-5472.CAN-08-2281.
[14] Herbst R, et al. Predictive correlates of response to the anti-PD-L1 antibody MPDL3280A in cancer patients. Nature 2014;515:563–7. https://doi.org/10.1038/nature14011.
[15] Tumeh P, et al. PD-1 blockade induces responses by inhibiting adaptive immune resistance. Nature 2014;515:568–71. https://doi.org/10.1038/nature13954.
[16] Muller M, Schouten R, Gooijer C, Baas P. Pembrolizumab for the treatment of non-small cell lung cancer. Expert Rev Anticancer Ther 2017;17. https://doi.org/10.1080/14737140.2017.1311791.
[17] Hugo W, et al. Genomic and transcriptomic features of response to anti-PD-1 therapy in metastatic melanoma. Cell 2017;168:542. https://doi.org/10.1016/j.cell.2017.01.010.
[18] Cho J-W, et al. Genome-wide identification of differentially methylated promoters and enhancers associated with response to anti-PD-1 therapy in non-small cell lung cancer. Exp Mol Med 2020;52:1–14. https://doi.org/10.1038/s12276-020-00493-8.
[19] Ascierto M, et al. The intratumoral balance between metabolic and immunologic gene expression is associated with anti-PD-1 response in patients with renal cell carcinoma. Cancer Immunol Res 2016;4. https://doi.org/10.1158/2326-6066.CIR-16-0072.
[20] Auslander N, et al. Robust prediction of response to immune checkpoint blockade therapy in metastatic melanoma. Nat Med 2018;24. https://doi.org/10.1038/s41591-018-0157-9.
[21] Du K, et al. Pathway signatures derived from on-treatment tumor specimens predict response to anti-PD1 blockade in metastatic melanoma. 6023-6023 Nat Commun 2021;12. https://doi.org/10.1038/s41467-021-26299-4.
[22] Gide T, et al. Distinct immune cell populations define response to anti-PD-1 monotherapy and Anti-PD-1/Anti-CTLA-4 combined therapy. e236 Cancer Cell 2019;35:238–55. https://doi.org/10.1016/j.ccell.2019.01.003.
[23] Kim S, et al. Comprehensive molecular characterization of clinical responses to PD-1 inhibition in metastatic gastric cancer. Nat Med 2018;24. https://doi.org/10.1038/s41591-018-0101-z.
[24] Van Allen EM, et al. Genomic correlates of response to CTLA-4 blockade in metastatic melanoma. Science 2015;350:207–11. https://doi.org/10.1126/science.aad0095.
[25] Jiang P, et al. Signatures of T cell dysfunction and exclusion predict cancer immunotherapy response. Nat Med 2018;24:1550–8. https://doi.org/10.1038/s41591-018-0136-1.

[26] Lee J, et al. Transcriptional downregulation of MHC class I and melanoma de-differentiation in resistance to PD-1 inhibition. Nat Commun 2020;11. https://doi.org/10.1038/s41467-020-15726-7.
[27] Lappalainen I, et al. The European genome-phenome archive of human data consented for biomedical research. Nat Genet 2015;47:692–5. https://doi.org/10.1038/ng.3312.
[28] Necchi A, et al. Atezolizumab in platinum-treated locally advanced or metastatic urothelial carcinoma: Post-progression outcomes from the phase II IMvigor210 study. Ann Oncol: J Eur Soc Med Oncol 2017;28. https://doi.org/10.1093/annonc/mdx518.
[29] Leek J, Johnson W, Parker H, Jaffe A, Storey J, The SVA. package for removing batch effects and other unwanted variation in high-throughput experiments. Bioinforma (Oxf, Engl) 2012;28:882–3. https://doi.org/10.1093/bioinformatics/bts034.
[30] Chang K, et al. The cancer genome atlas pan-cancer analysis project. Nat Genet 2013;45:1113–20. https://doi.org/10.1038/ng.2764.
[31] Castanza AS, et al. Extending support for mouse data in the Molecular Signatures Database (MSigDB). Nat Methods 2023. https://doi.org/10.1038/s41592-023-02014-7.
[32] Tibshirani R. Regression shrinkage and selection via the lasso. J R Stat Soc: Ser B (Methodol) 1996;58:267–88. https://doi.org/10.1111/j.2517-6161.1996.tb02080.x.
[33] Yu G, Wang L-G, Han Y, He Q-Y. clusterProfiler: an R package for comparing biological themes among gene clusters. OMICS 2012;16:284–7. https://doi.org/10.1089/omi.2011.0118.
[34] Yoshihara K, et al. Inferring tumour purity and stromal and immune cell admixture from expression data. Nat Commun 2013;4:2612. https://doi.org/10.1038/ncomms3612.
[35] Racle J, Gfeller D. EPIC: a tool to estimate the proportions of different cell types from bulk gene expression data. Methods Mol Biol 2120 2020:233–48. https://doi.org/10.1007/978-1-0716-0327-7_17.
[36] Becht E, et al. Estimating the population abundance of tissue-infiltrating immune and stromal cell populations using gene expression. Genome Biol 2016;17. https://doi.org/10.1186/s13059-016-1070-5.
[37] Miao YR, et al. ImmuCellAI: a unique method for comprehensive T-cell subsets abundance prediction and its application in cancer immunotherapy. Adv Sci 2020;7:1902880. https://doi.org/10.1002/advs.201902880.
[38] Newman A, et al. Robust enumeration of cell subsets from tissue expression profiles. Nat Methods 2015;12. https://doi.org/10.1038/nmeth.3337.
[39] Aran D. Bioinformatics for Cancer Immunotherapy: Methods and Protocols (ed Sebastian Boegel). US: Springer; 2020. p. 263–76.
[40] Li T, et al. TIMER: a web server for comprehensive analysis of tumor-infiltrating immune cells. Cancer Res 2017;77:e108–10. https://doi.org/10.1158/0008-5472.CAN-17-0307.
[41] Yi M, Nissley D, Stephens R. ssGSEA score-based Ras dependency indexes derived from gene expression data reveal potential Ras addiction mechanisms with possible clinical implications. Sci Rep 2020;10. https://doi.org/10.1038/s41598-020-66986-8.
[42] Thorsson V, et al. The immune landscape of cancer. Immunity 2019;51:411–2. https://doi.org/10.1016/j.immuni.2019.08.004.
[43] Bagaev A, et al. Conserved pan-cancer microenvironment subtypes predict response to immunotherapy. Cancer Cell 2021;39. https://doi.org/10.1016/j.ccell.2021.04.014.
[44] Sing T, Sander O, Beerenwinkel N, Lengauer T. ROCR: visualizing classifier performance in R. Bioinforma (Oxf, Engl) 2005;21:3940–1. https://doi.org/10.1093/bioinformatics/bti623.
[45] Therneau, T. & Grambsch, P. Modeling Survival Data: Extending the Cox Model. (2013).
[46] Viechtbauer W. Conducting meta-analyses in r with the metafor package. J Stat Softw 2010;36. https://doi.org/10.18637/jss.v036.i03.
[47] Team, R.C.R: A language and environment for statistical computing (2014).
[48] Chen S, Zhang L, Huang M, Liang Y, Wang Y. A tumor-associated endothelial signature score model in immunotherapy and prognosis across pan-cancers. Front Pharm 2023;14:1190660. https://doi.org/10.3389/fphar.2023.1190660.
[49] Zhao Y, et al. IL-21 is an accomplice of PD-L1 in the induction of PD-1-dependent treg generation in head and neck cancer. ARTN 64829310.3389/fonc.2021.648293 Front Oncol 2021;11. ARTN 64829310.3389/fonc.2021.648293.
[50] Racle, J. & Gfeller, D. Vol. 2120 233–248 (2020).
[51] Thompson JC, et al. Gene signatures of tumor inflammation and epithelial-to-mesenchymal transition (EMT) predict responses to immune checkpoint blockade in lung cancer with high accuracy. Lung Cancer 2020;139:1–8. https://doi.org/10.1016/j.lungcan.2019.10.012.
[52] Auslander N, et al. Robust prediction of response to immune checkpoint blockade therapy in metastatic melanoma (vol 24, pg 1545, 2018). 1942-1942 Nat Med 2018;24. https://doi.org/10.1038/s41591-018-0247-8.
[53] Hugo, W. *et al.* Genomic and Transcriptomic Features of Response to Anti-PD-1 Therapy in Metastatic Melanoma (vol 165, pg 35, 2016). *Cell* **168**, 542–542, doi:10.1016/j.cell.2017.01.010 (2017).
[54] Dominguez CX, et al. Single-cell RNA sequencing reveals stromal evolution into LRRC15+ myofibroblasts as a determinant of patient response to cancer immunotherapy. Cancer Discov 2020;10:232–53. https://doi.org/10.1158/2159-8290.CD-19-0644.
[55] Yang S, et al. Identification of a prognostic immune signature for cervical cancer to predict survival and response to immune checkpoint inhibitors. ARTN e165909410.1080/2162402X.2019.1659094 Oncoimmunology 2019;8. ARTN e165909410.1080/2162402X.2019.1659094.
[56] Shukla SA, et al. Cancer-germline antigen expression discriminates clinical outcome to CTLA-4 blockade. 624-+ Cell 2018;173. https://doi.org/10.1016/j.cell.2018.03.026.
[57] Jiang P, et al. Signatures of T-cell dysfunction and exclusion predict cancer immunotherapy response. Cancer Immunol Res 2019;7. https://doi.org/10.1158/2326-6074.Cricimteatiaacr18-B077.
[58] Patil N, et al. Intratumoral plasma cells predict outcomes to Pd-L1 blockade in non-small cell lung cancer. A456-A456 J Immunother Cancer 2022;10. https://doi.org/10.1136/jitc-2022-SITC2022.0435.
[59] Robert C, et al. Nivolumab in Previously Untreated Melanoma without BRAF Mutation. N Engl J Med 2014;372:320–30. https://doi.org/10.1056/NEJMoa1412082.
[60] Aran D, Sirota M, Butte AJ. Systematic pan-cancer analysis of tumour purity. Nat Commun 2015;6:8971. https://doi.org/10.1038/ncomms9971.
[61] Liu Z, Li M, Jiang Z, Wang X. A Comprehensive Immunologic Portrait of Triple-Negative Breast Cancer. Transl Oncol 2018;11:311–29. https://doi.org/10.1016/j.tranon.2018.01.011.
[62] Ribas A, Wolchok JD. Cancer immunotherapy using checkpoint blockade. Sci (N Y, N Y) 2018;359:1350–5. https://doi.org/10.1126/science.aar4060.
[63] Robert C, et al. Pembrolizumab versus ipilimumab in advanced melanoma (KEYNOTE-006): post-hoc 5-year results from an open-label, multicentre, randomised, controlled, phase 3 study. Lancet Oncol 2019;20. https://doi.org/10.1016/S1470-2045(19)30388-2.
[64] Bownes RJ, et al. On-treatment biomarkers can improve prediction of response to neoadjuvant chemotherapy in breast cancer. ARTN 7310.1186/s13058-019-1159-3 Breast Cancer Res 2019;21. ARTN 7310.1186/s13058-019-1159-3.
[65] Turnbull AK, et al. Accurate prediction and validation of response to endocrine therapy in breast cancer. 2270-U2272 J Clin Oncol 2015;33. https://doi.org/10.1200/Jco.2014.57.8963.
[66] Duffy M, Crown J. Biomarkers for predicting response to immunotherapy with immune checkpoint inhibitors in cancer patients. clinchem.2019.303644 Clin Chem 2019;65. https://doi.org/10.1373/clinchem.2019.303644.
[67] Binnewies M, et al. Understanding the tumor immune microenvironment (TIME) for effective therapy. Nat Med 2018;24. https://doi.org/10.1038/s41591-018-0014-x.
[68] Parrish-Novak J, et al. Interleukin 21 and its receptor are involved in NK cell expansion and regulation of lymphocyte function. Nature 2000;408:57–63. https://doi.org/10.1038/35040504.
[69] Tian Y, et al. A context-dependent role for il-21 in modulating the differentiation, distribution, and abundance of effector and memory CD8 T cell subsets. J Immunol (Baltim, Md: 1950) 2016;196. https://doi.org/10.4049/jimmunol.1401236.
[70] Seo H, et al. IL21 therapy combined with PD-1 and tim-3 blockade provides enhanced NK cell antitumor activity against mhc class i-deficient tumors. canimm.0708.2017 Cancer Immunol Res 2018;6. https://doi.org/10.1158/2326-6066.CIR-17-0708.
[71] Deng S, et al. Targeting tumors with IL-21 reshapes the tumor microenvironment by proliferating PD-1intTim-3–CD8+ T cells. JCI Insight 2020;5. https://doi.org/10.1172/jci.insight.132000.